Received: 23 March 2023 | Revised: 17 May 2023 | Accepted: 21 May 2023

DOI: 10.1002/pls2.10097

RESEARCH ARTICLE

SPE POLYMERS WILEY

Development of poly(vinylidene fluoride)/thermoplastic polyurethane/carbon black-polypyrrole composites with enhanced piezoelectric properties

Mayara C. Bertolini[1,2] | **Nico Zamperlin**[1] | **Guilherme M. O. Barra**[2] | **Alessandro Pegoretti**[1,3]

[1]Department of Industrial Engineering, University of Trento, Trento, Italy

[2]Department of Mechanical Engineering, Universidade Federal de Santa Catarina, Florianópolis, Brazil

[3]National Interuniversity Consortium of Materials Science and Technology (INSTM), Florence, Italy

Correspondence
Alessandro Pegoretti, Department of Industrial Engineering, University of Trento, Trento, Italy.
Email: alessandro.pegoretti@unitn.it

Funding information
Conselho Nacional de Desenvolvimento Científico e Tecnológico; Italian Ministry for University and Research (MUR), Grant/Award Number: L.232/2016

Abstract

Poly(vinylidene fluoride)/thermoplastic polyurethane (PVDF/TPU) composites filled with carbon-black polypyrrole were prepared via melt compounding followed by compression molding and fused filament fabrication. CB-PPy was added to the blends from 0 up to 15% to possible act as nucleating filler for PVDF β phase in order to increase its piezoelectric response. The influence of blending PVDF and TPU and of the addition of CB-PPy on the overall crystallinity, content of β phase, and piezoelectric response of composites were investigated by differential scanning calorimetry (DSC), Fourier-transformed infrared spectroscopy (FTIR), X-ray diffraction (XRD) and determination of the piezoelectric coefficient (d_{33}). It was found that the addition of TPU to PVDF induced an increase of the crystallinity degree and content of β phase in PVDF. Moreover, although the degree of crystallinity of the composites decreased with the addition of CB-PPy, the percentage of β phase in PVDF was increased. This effect is more significant in samples with filler concentration higher than 6 wt%. As expected, the d_{33} of the composites increased as the content of the β phase increased. Furthermore, 3D printed samples displayed lower content of β phase and reduced piezoelectric responses when compared to compression molded samples with same composition.

KEYWORDS

fused filament fabrication, nanofiller, piezoelectric, polymer blend, PVDF, β phase

1 | INTRODUCTION

The piezoelectric effect is based on the generation of electrical potential variations as response to externally applied mechanical strains. Therefore, when a mechanical force is applied, the electric dipole moments separate and the opposite surfaces of a flat sample become positively and negatively charged creating a piezopotential that leads to a flow of the free electrons through the external circuit to reach a balanced state again.[1–5] Piezoelectric materials have been employed in various technological applications including sensors, actuators, and energy harvesting devices.[1,6,7] The energy conversion efficiency of these materials can be assessed by the

piezoelectric constant or piezoelectric charge coefficient (d_{33}) that refers to the materials electric response to an applied force in units of electrical charge (in Coulomb) per unit of force (in Newton).[2,7,8] Among piezoelectric materials, piezoelectric ceramics present a high d_{33} constant but suffer from low flexibility and brittleness making them not suitable for flexible electronic devices. Moreover, the preparation of ceramics requires specific equipment for high processing temperature.[1,2,9] For this reason, several studies have been carried out on the development of flexible piezoelectric materials based on piezoelectric polymers or polymer composites, which display higher flexibility and an easier integration to functional devices even though their piezoelectric coefficient d_{33} is not as high as for inorganic materials.[2,8,10] A potential piezoelectric polymer is PVDF which is well known for its substantial higher dielectric constant around 10 when compared to the usual 2–5 of other polymers[11] and offers the advantages of nontoxicity, lightweight, flexibility, good biocompatibility, good processability, low cost, and easy integration to devices.[1,6,9,10]

PVDF is a thermoplastic semi-crystalline polymer composed of repeated units of vinylidene difluoride. Depending on its chain conformations, PVDF can exist in five crystalline phases: α, β, γ, δ, and ε.[1,12–14] The nonpolar α phase is predominant in commercially available PVDF because it is thermodynamically more stable than the other phases.[12,15] However, PVDF piezoelectric properties are related to the all transplanar zigzag TTTT and trans-gauche T3GT3G′ conformations of the polar phases β and γ,[10] respectively, being β the one with the higher dipole moment and, therefore, the higher piezoelectric response.[1,5,7,8,12,13,15–19] In this framework, the main challenge is to convert the nonpolar α phase of PVDF in the β phase. Several techniques have been developed to increase the fraction of β phase in PVDF polymers to enhance its piezoelectric properties such as mechanical stretching, high electrical field poling, crystallization under high pressure, polymer blending, electrospinning, thermal annealing, addition of nanofillers, hot pressing, and 3D printing.[1,5,7,9,10,12–14,16,17,20–23]

The piezoelectric properties of PVDF are related not only to the polymer phase, but also to the degree of crystallinity, microstructure and processing conditions.[24] For instance, Seena et al[14] succeeded in raising the overall polar phases of PVDF samples, specially the β phase, by proper hot pressing conditions. Besides the traditional manufacturing methods, 3D printing is a promising technology for preparing materials with complex 3D geometries and technological functionalities.[9,16] In this context, the fused filament fabrication (FFF) technique has a great potential to produce components with multifunctional response, including piezoelectricity.[25] Nevertheless, processing PVDF via FFF is still a challenge because of its large thermal expansion coefficient that leads to warping deformation and its elevated shrinking during crystallization.[26,27] In addition, PVDF printed parts present low stretchability and low elongation at break thus limiting their applications.

In this context, blending PVDF with thermoplastic polyurethane (TPU) could be an efficient way to prepare materials with an excellent combination between the piezoelectric response of PVDF and the elastomeric properties of TPU.[6,28,29] Previous researches showed that hybrid materials of PVDF and TPU offers unique advantages of mechanical properties, such as stretchability and flexibility, and pyroelectric/piezoelectric properties.[4,6,28–31]

Furthermore, the dispersion of nanofillers is an interesting strategy to induce the formation of an electroactive phase and enhance piezoelectric properties of PVDF.[5,10,12,13,16,20,21,23,25,32] Among the reported nanofillers, carbon nanofillers have been mostly used because of their high surface area, good mechanical properties, elevated electron transport properties, and superior polymer-filler interfacial interactions.[5,13,14] For instance, Fakhri et al[12] developed PVDF composites containing graphene oxide doped with Au and Cu (GO/Au and GO/Cu) with high content of electroactive phases and high dielectric constant. Moreover, Georgousis et al[33] reported an enhancement of the β phase content in PVDF composites by adding 6 wt% and 8 wt% of CNT via melting compounding.

Therefore, this work investigates the development of PVDF/TPU composites filled with carbon black (CB) doped with polypyrrole to increase the content of PVDF β phase and to enhance the piezoelectric properties of the resulting composites. Two fabrication methods were investigated: melt compounding followed by compression molding and extrusion followed by FFF. To our best knowledge, there are no similar studies concerning the development of materials filaments comprising polymer blends of PVDF/TPU and conductive filler.

2 | EXPERIMENTAL

2.1 | Materials

The selected PVDF with a melting temperature of 165–175°C, a density of 1.78 g cm^{-3} and an electrical conductivity of 10^{-13} S cm^{-1} was purchased from Amboflon®. The selected TPU is a Desmopan® DP 6064 A from Covestro with a melting temperature of 200–220°C, a relative density of 1.09 g cm^{-3} and an electrical conductivity of 10^{-11} S cm^{-1}. A CB-PPy containing 80 wt% of CB with a density of 2.22 g cm^{-3} and an electrical conductivity of 3×10^{1} S cm^{-1} was purchased from Sigma Aldrich.

TABLE 1 Composition of PVDF/TPU/CB-PPy composites.

PVDF/TPU 38/62 vol%	PVDF/TPU 50/50 vol%
CB-PPy (%)	CB-PPy (%)
3	1
5	2
6	3
7	5
10	6
15	10

Abbreviations: PVDF, poly(vinylidene fluoride); TPU, thermoplastic polyurethane.

TABLE 2 Composition of 3D printed composites.

PVDF/TPU 38/62 vol%
CB-PPy (%)
5
6
PVDF/TPU 50/50 vol%
CB-PPy (%)
10

2.2 | Sample preparation

2.2.1 | Preparation of PVDF/TPU/CB-PPy composites

PVDF/TPU/CB-PPy composites were produced using two different PVDF/TPU blend compositions as matrices, PVDF/TPU 38/62 vol% and PVDF/TPU 50/50 vol%. The final composition of the composites is displayed in Table 1. Composites were produced by melt compounding using a Thermo-Haake Polylab 600 Rheomix internal mixer with counter-rotating rotors and 50 cm^3 of internal volume. Before mixing, the materials were dried overnight at 60°C. Then, previous calculated amount of PVDF and TPU were mixed at 180°C and a rotor speed of 50 rpm and after 2 min CB-PPy was introduced and mixed for more 13 min.

2.2.2 | Compression molding

The prepared composites were compression molded in squares plates of 120 mm^2 with 2 mm of thickness using a Carver Laboratory press at 180°C under a pressure of 3.9 MPa for 10 min. Compression molded samples were cut in specific formats for different characterization. Moreover, samples in film format were also prepared by compression molding at a pressure of 3.9 MPa for 5 min at 180°C using a BOVENAU P15 ST hydraulic press.

2.2.3 | Fused filament fabrication

According to the results from our previous investigations,[30,31] three compositions (see Table 2) were selected to be printed via FFF. For the preparation of the filaments, the composites prepared by melt compounding were immersed in liquid nitrogen, grinded and then extruded in filaments with a diameter of 1.75 ± 0.10 mm using a single screw extruder Friul Filiere SpA model Estru 13 operating at 30 rpm with four temperature zones at 130, 170, 175, and 180°C (die). The extruded filaments were collected on a rolling belt at 20 mm s^{-1}.

The filaments were used for the 3D-printing of circular disks with a diameter of 15 mm and 2 mm in thickness by a Sethi S3 3D printer based on the FFF technology. The following printing parameters were settled using the open source software Slic3r: nozzle temperature 230°C; nozzle diameter 0.4 mm; nozzle speed 40 mm s^{-1}; printing platform temperature 40°C; layer height 0.2 mm; object infill rectangular 100% and raster angle +45°/−45° (horizontal alternate direction H45).

2.3 | Testing techniques

Differential scanning calorimetry (DSC) measurements were conducted on a Perkin Elmer JADE DSC calorimeter at a heating rate of 10°C min^{-1} from 20 to 250°C under a nitrogen flow of 100 mL min^{-1}. Samples of about 10 mg were analyzed. The melting temperature of the composites was measured and the crystallinity content (X_c) of PVDF was calculated according to the following equation:

$$X_c = \frac{\Delta H_m}{\Delta H_m^* \emptyset} \times 100\%$$

where ΔH_m is the melting enthalpy of the specimen obtained by the DSC measurement, ΔH_m^* is the melting enthalpy of pure crystalline PVDF (104.5 J g^{-1} [7,25,28]) and $\emptyset$ is the weight fraction of PVDF in the composites.

The chemical structure, interaction between components and crystalline phases of PVDF were evaluated by Fourier transform infrared (FTIR) in the attenuated total reflectance (ATR) mode using a ZnSe crystal by an Agilent Cary 660 spectrometer. The scans were performed in the range of 4000–650 cm^{-1} and the samples were analyzed in the film format.

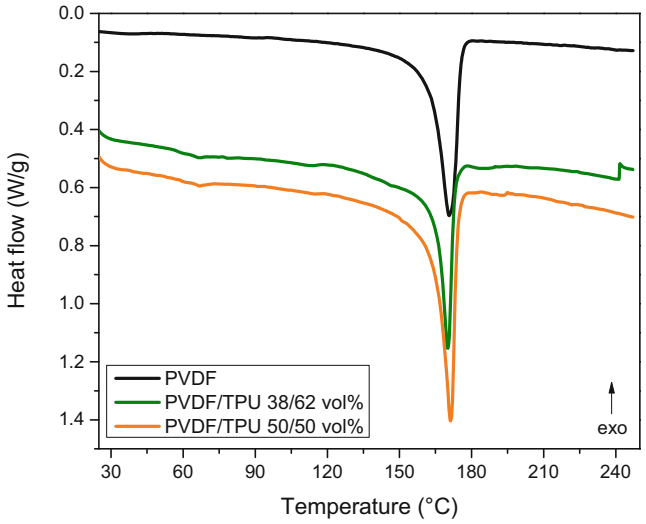

FIGURE 1 Heat flow curves as a function of temperature for neat poly(vinylidene fluoride) (PVDF) and PVDF/thermoplastic polyurethane blends.

The X-ray diffraction patterns (XRD) were obtained from an Italstructures IPD3000 diffractometer equipped with a standard sealed-tube source of Copper [Cu] anode, a multilayer flat monochromator on the incident beam selecting CuKa and a Dectris Mythen 1 K detector with 2θ angles ranging from 10 to 120°.

The piezoelectric response of the samples was assessed using a piezolelectric d_{33} meter OKD3-2000-F10N purchased from PolyK Technologies. An oscillating force of 0.25 N was applied to the specimens with a fixed frequency of 110 Hz and three different static clamping forces of 1, 2, and 4 N were applied to evaluate the effect of the applied load. The d_{33} constant (pC/N) was measured by reading the surface charge on the electrode. Nine measurements were performed on three different spots of each sample in film format.

3 | RESULTS AND DISCUSSION

3.1 | Differential scanning calorimetry

The DSC thermograms for neat PVDF and for PVDF/TPU 38/62 vol% and 50/50 vol% blends are displayed in Figure 1. In addition, Table 3 summarize the melting temperature (T_m), the melting enthalpy (ΔH_m), the weight fraction of PVDF (∅) in the samples and crystallinity content (X_c) values of the materials.

The results show that the melting temperature (T_m) of the mixtures slightly decreases with the addition of TPU to PVDF due to the poor compatibility between the two polymers, which confirms the results already described in our previous work.[30] According to previous studies, the decrease in the melting temperature is more significant in highly compatible blends. In fact, Bera et al[28] reported a considerably reduction in the T_m of PVDF for poly(vinylidene fluoride)/poly(methyl methacrylate) (PVDF/PMMA) 70/30 compatible blends (i.e., 27°C) than for PVDF/TPU 70/30 blends.

Moreover, from the calculation of the crystallinity content (X_c) is possible to notice that blending PVDF with TPU leads to an increase of the degree of crystallinity of the samples supporting the claim that the addition of TPU to the blends can assist to the crystallization of PVDF chains.

Furthermore, Figure 2 presents the curves of heat flow as a function of temperature for PVDF/TPU/CB-PPy 38/62 vol% and 50/50 vol% composites comprising various amount of conductive filler. In addition, the melting temperature (T_m), the melting enthalpy (ΔH_m), the weight fraction of PVDF (∅) in the samples, and crystallinity content (X_c) values of the composites are summarized in Table 3. Overall, the addition of the conductive filler CB-PPy decreases the melting temperature and the percentage of crystallinity of the mixtures indicating that the particles of the filler can probably hinder the crystallization of PVDF chains.

Moreover, it is interesting to notice that a double melting peak was found for PVDF/TPU/CB-PPy 10% (38/62 vol%) and PVDF/TPU/CB-PPy 5% (50/50 vol%) composites, which can be explained by the formation of imperfect crystallites, the formation of two distinct types of crystals or melt recrystallization.[34] While a single melting peak is generally associated to more homogeneous lamellae that melt simultaneously during the heating process.

3.2 | Fourier transform infrared

FTIR analysis was performed in order to investigate the chemical structure of PVDF and TPU, their interaction in the PVDF/TPU 38/62 vol% and 50/50 vol% blends, to estimate the crystalline phases of PVDF and the effect of material composition and processing technique in PVDF β phase.

Figure 3 shows the FTIR spectra of neat PVDF, neat TPU, PVDF/TPU 38/62 vol% and 50/50 vol% blends fabricated by compression molding and a zoom of the 1750–650 cm^{-1} region is also provided. For neat PVDF, the peaks at 870 and 1402 cm^{-1} correspond to C—F stretching vibration and the peak at 1177 cm^{-1} corresponds to C—C bond.[6,35] The band at 762 cm^{-1} is related to CH_2 in-plane bending, while the bands at 795 and 974 cm^{-1} can be attributed to CH_2 rocking and twisting, respectively.[24]

TABLE 3 Summary of melting temperature values, melting enthalpy values, PVDF weight fraction, and crystallinity content for neat PVDF and PVDF/TPU/CB-PPy composites.

Sample	T_m (°C)	ΔH_m (J g^{-1})	∅	X_C (%)
PVDF	172.6	51.9	1	49.6
PVDF/TPU 38/62 vol%				
CB-PPy (%)	T_m (°C)	ΔH_m (J g^{-1})	∅	X_C (%)
0	170.2	35.00	0.5	67.0
3	168.6	29.96	0.485	59.1
5	169.2	30.61	0.475	61.7
10	166.6/172.3	28.58	0.45	60.8
PVDF/TPU 50/50 vol%				
CB-PPy (%)	T_m (°C)	ΔH_m (J g^{-1})	∅	X_C (%)
0	171.3	48.22	0.620	74.4
1	167.9	36.46	0.614	56.8
5	165.7/170.9	35.23	0.589	57.2
10	175.0	34.01	0.558	58.3

Abbreviations: PVDF, poly(vinylidene fluoride); TPU, thermoplastic polyurethane.

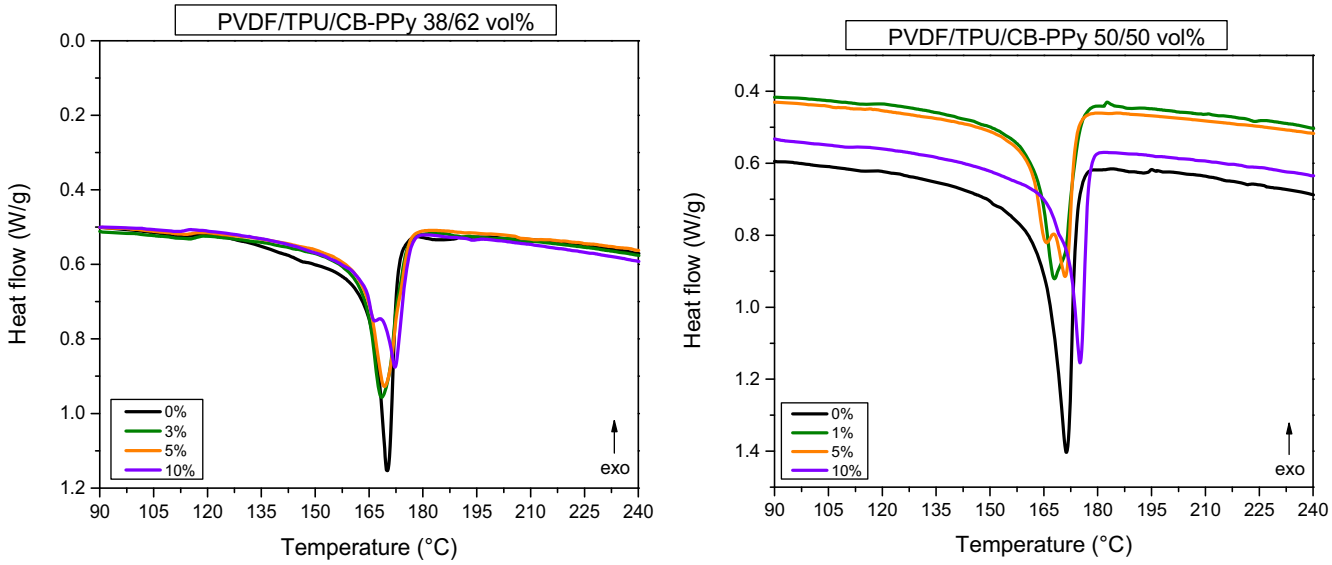

FIGURE 2 Heat flow curves as a function of temperature for PVDF/TPU/CB-PPy composites comprising various amount of filler. PVDF, poly(vinylidene fluoride); TPU, thermoplastic polyurethane

Moreover, the presence of some peaks reported in the literature as characteristics of PVDF α phase can be seen at 762, 795, 854, 974, and 1424 cm^{-1}.[7,12,15,18,24,25,28] On the other hand, the peaks corresponding to PVDF β phase are found at 840, 1073, and 1278 cm^{-1}.[6,14,15,18,25,35] For neat TPU, the peak at 3301 cm^{-1} is attributed to hydrogen-bonded N—H stretching. The bands at 2917 and 2915 cm^{-1} corresponds to symmetric and asymmetric axial deformation of aliphatic CH_2. In addition, the band at 1728 cm^{-1} is related to free carbonyl stretching vibration, while the band at 1702 cm^{-1} is related to hydrogen bonded carbonyl groups.[24,28,36] The peaks at 1978, 1529, 1309, and 1222 cm^{-1} are associated to C—O—C bond, C—N stretching, N—H bending and aliphatic C—O stretching, respectively.[28] Furthermore, for the blends PVDF/TPU 38/62 vol% and 50/50 vol%, the FTIR spectra present the main absorption peaks of both components because they are not chemically bonded and the phases of the blend are not mutually soluble.

Furthermore, the FTIR peaks at 762 and 840 cm^{-1} (characteristics of α and β phases) were used to calculate the percentage of β phase in PVDf, F(β), according to the following equation[6,12,15,25]:

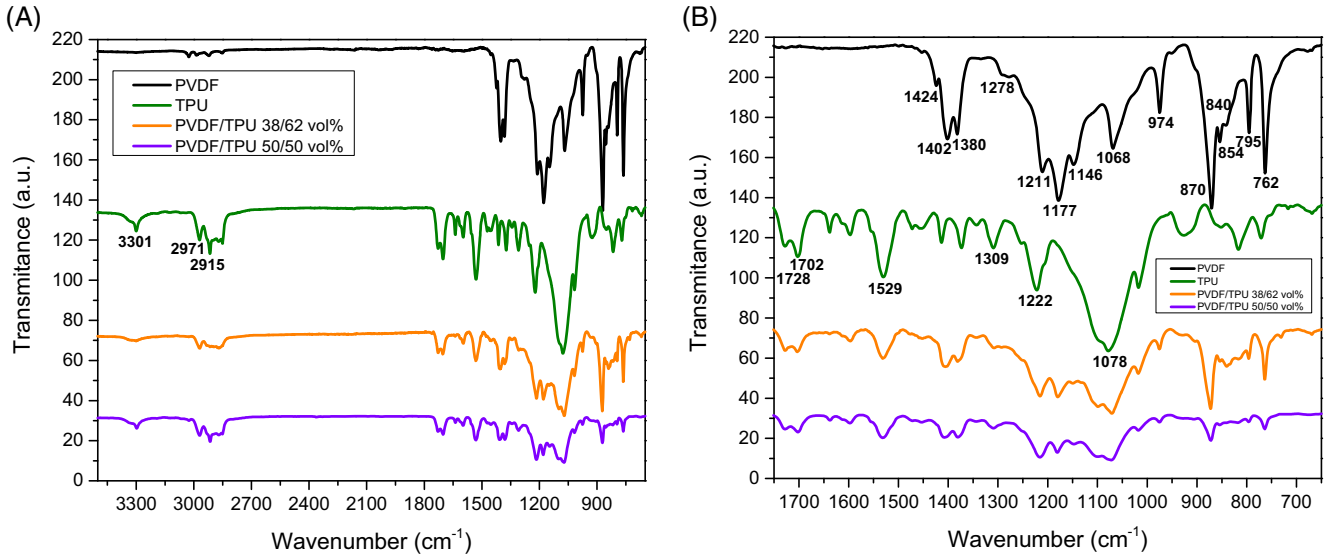

FIGURE 3 (A) Fourier-transformed infrared spectroscopy (FTIR) spectra of neat poly(vinylidene fluoride) (PVDF), neat thermoplastic polyurethane (TPU) and PVDF/TPU 38/62 vol% and 50/50 vol% blends prepared by compression molding; and (B) zoom in the FTIR spectra at the region of 1750–650 cm^{-1}.

Sample	λ_α (cm^{-1})	λ_β (cm^{-1})	A_α	A_β	$F(\beta)$ (%)
Neat PVDF	762	840	0.403	0.204	31
PVDF/TPU 38/62 vol%	762	840	0.115	0.092	41
PVDF/TPU 50/50 vol%	762	840	0.017	0.009	33

Abbreviations: PVDF, poly(vinylidene fluoride); TPU, thermoplastic polyurethane.

TABLE 4 Values of λ, A, and $F(\beta)$ for neat PVDF and PVDF/TPU 38/62 vol% and 50/50 vol% blends.

$$F(\beta) = \frac{A_\beta}{(K_\beta/K_\alpha)A_\alpha + A_\beta}$$

where $F(\beta)$ is the β phase content, A_α and A_β are the absorbance intensities and K_α and K_β are the absorption coefficients at 762 and 840 cm^{-1}, respectively, with values of 6.1×10^4 cm^2 mol^{-1} and 7×10^4 cm^2 mol^{-1}.[15,25] The calculated $F(\beta)$ in neat PVDF and in the PVDF/TPU blends are presented in Table 4. The results show that the content of PVDF β phase increases when TPU is added to the blend. In fact, the $F(\beta)$ for neat PDVF is 31% and it increases to 41% in the PVDF/TPU 38/62 vol% blend and to 33% in the PVDF/TPU 50/50 vol% blend. This indicates that polymer blending can contribute to the phase transformation of PVDF as described in some studies.[21,22,37]

The contribution of the addition of the conductive filler CB-PPy on the phase transformation of PVDF was also evaluated by the FTIR analysis. Previous studies describe the addition of carbonaceous fillers to PVDF composites as a strategy to improve the formation of its β phase.[5,10,12,13,16,20,32,33] In this context, Wu et al[20] state that the addition of the conductive filler CB in PVDF composites assisted its β phase formation since CB acted as a nucleating agent.

The measured $F(\beta)$ values for the PVDF/TPU/CB-PPy 38/62 vol% and 50/50 vol% compression molded composites comprising various amount of CB-PPy are displayed in Table 5. The results illustrate that the addition of high amount of CB-PPy (i.e., 5% or more) improves the content of β phase in PVDF. In fact, it is possible to observer that composites comprising 6% and 10% of CB-PPy display higher β phase content, from 50% up to 61%, for both composites. Thus, endorsing the claim that the addition of the filler can assist the formation of β phase in PVDF. Although the DSC results show that the overall crystallinity of the samples decreases with the addition of CB-PPy, the percentage of the β crystalline phase increases.

In addition, the influence of the processing method on the formation of the β phase in PVDF was also investigated. Table 6 shows a comparison between the $F(\beta)$ in compression molded and 3D printed samples with same composition. The content of β phase in PVDF was found to be lower for all samples fabricated by FFF when compared to the samples with same composition prepared by compression molding. It may happen because the

TABLE 5 Values of λ, A, and $F(\beta)$ for PVDF/TPU/CB-PPy 38/62 vol% and 50/50 vol% composites containing various amount of CB-PPy prepared by compression molding.

PVDF/TPU 38/62 vol%					
CB-PPy (%)	**λ_α (cm^{-1})**	**λ_β (cm^{-1})**	**A_α**	**A_β**	**$F(\beta)$ (%)**
0	762	840	0.115	0.092	41
3	763	840	0.029	0.023	41
5	762	837	0.163	0.152	45
6	764	835	0.018	0.021	50
10	763	835	0.023	0.042	61
PVDF/TPU 50/50 vol%					
CB-PPy (%)	**λ_α (cm^{-1})**	**λ_β (cm^{-1})**	**A_α**	**A_β**	**$F(\beta)$ (%)**
0	763	840	0.017	0.010	33
1	762	841	0.047	0.026	32
3	763	840	0.023	0.013	32
6	764	840	0.237	0.289	52
10	764	833	0.027	0.040	57

Abbreviations: PVDF, poly(vinylidene fluoride); TPU, thermoplastic polyurethane.

TABLE 6 Comparison between $F(\beta)$% of compression molded and 3D printed PVDF/TPU/CB-PPy composites.

PVDF/TPU 38/62 vol%		
CB-PPy (%)	**$F(\beta)$ CM (%)**	**$F(\beta)$ 3D (%)**
0	41	37
5	45	43
6	50	43
PVDF/TPU 50/50 vol%		
CB-PPy (%)	**$F(\beta)$ CM (%)**	**$F(\beta)$ 3D (%)**
10	57	49

Abbreviations: PVDF, poly(vinylidene fluoride); TPU, thermoplastic polyurethane.

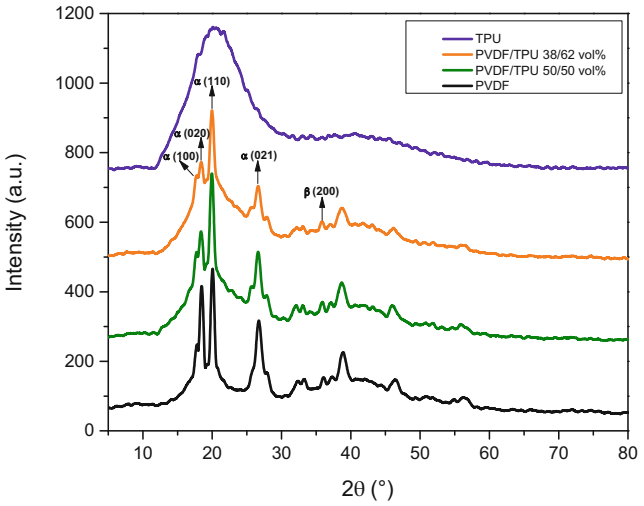

FIGURE 4 X-ray diffraction patterns of neat poly(vinylidene fluoride) (PVDF), neat thermoplastic polyurethane (TPU) and PVDF/TPU 38/62 vol% and 50/50 vol% blends prepared by compression molding.

thermal effect of processing techniques that can affect the polarization of PVDF crystalline phases decreasing the amount of β phase.[18]

3.3 | X-ray diffraction

In order to further evaluate the influence of the addition of TPU and CB-PPy and also the processing techniques on the PVDF crystalline phases, XRD measurements were carried out for neat PVDF, neat TPU, PVDF/TPU 38/62 vol%, and 50/50 vol% blends and composites containing various amount of CB-PPy. The XRD peaks displayed in Figure 4 show the characteristic peaks of the neat polymers. The broad and diffuse peak at 20.5° of neat TPU is characteristic of a completely amorphous material and it is associated to both hard and soft domains of TPU. Different from TPU, PVDF presents a substantial degree of crystallinity resulting in the diffraction peaks at 17.7°, 18.4°, 20.0°, and 26.6° related to the (100), (020), (110), and (021) diffraction planes that are commonly associated to the nonpolar α phase of PVDF.[12,13,18,38] On the other hand, the peak that corresponds to the polar β phase of PVDF can be found at 36.0 (200).[13,18] Although previous studies show that main peak corresponding to the PVDF β phase is at 20.6°,[6,18] it is difficult to relate this peak only to the β phase by XRD patterns since α, β and γ phases have an intense diffraction peak around 20°.[16]

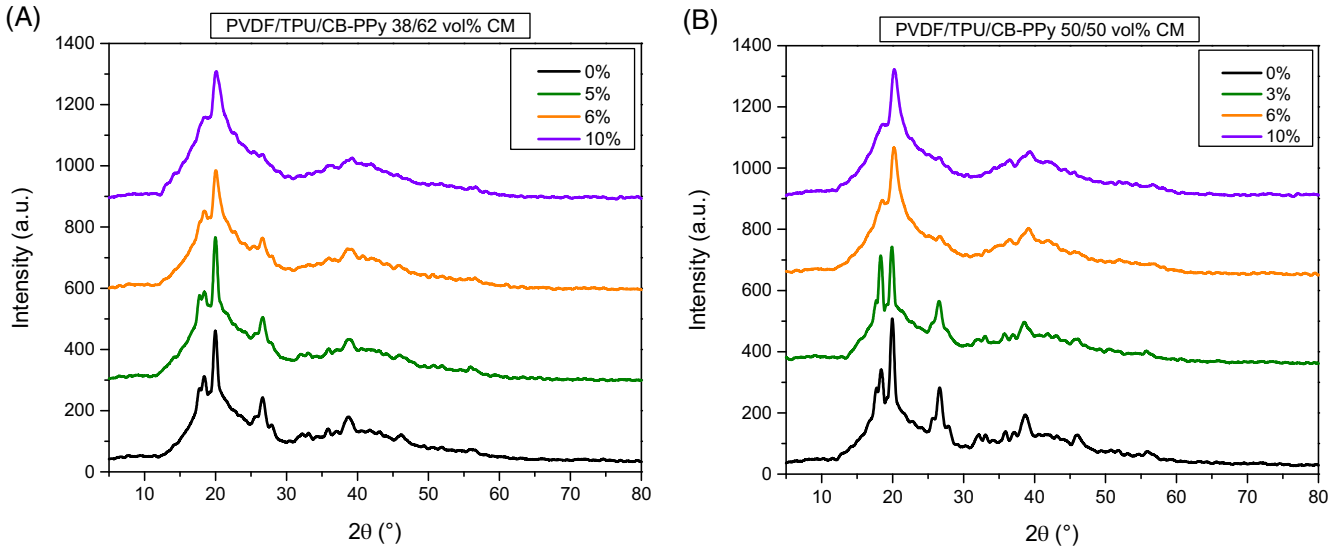

FIGURE 5 X-ray diffraction patterns of (A) PVDF/TPU/CB-PPy 38/62 vol% and (B) PVDF/TPU/CB-PPy 50/50 vol% composites prepared by compression molding comprising various amount of CB-PPy. PVDF, poly(vinylidene fluoride); TPU, thermoplastic polyurethane

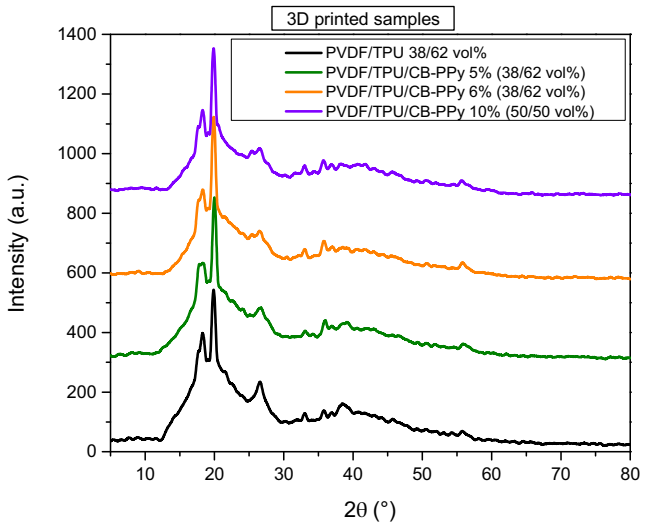

FIGURE 6 X-ray diffraction patterns of PVDF/TPU/CB-PPy composites with various content of CB-PPy prepared by fused filament fabrication. PVDF, poly(vinylidene fluoride); TPU, thermoplastic polyurethane

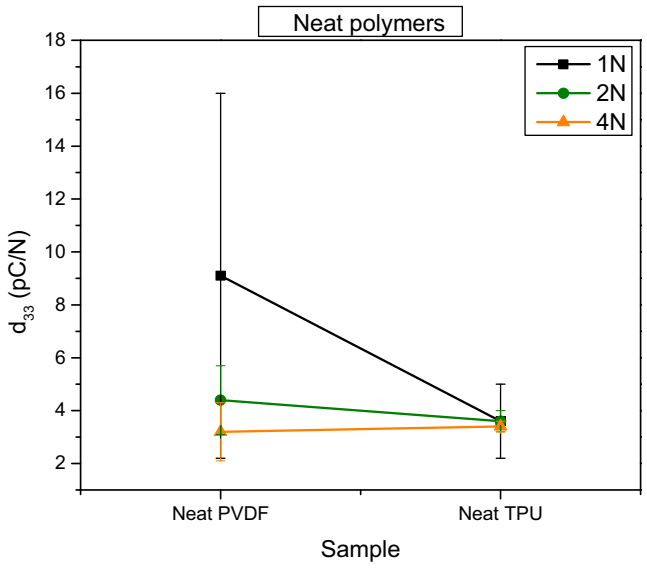

FIGURE 7 Piezoelectric coefficient (d_{33}) of neat poly(vinylidene fluoride) (PVDF) and neat thermoplastic polyurethane (TPU) samples prepared by compression molding.

Moreover, the diffraction patterns of the compression molded blends composed of PVDF/TPU 38/62 vol% and 50/50 vol% are a combination of the XRD patterns of the neat polymers, as expected. In addition, the peak related to PVDF α phase found at 18.4° seems to be diminished with the addition of TPU to PVDF, while the peak corresponding to the β phase of PVDF found at 36.0° was slightly increased. These results corroborate to those obtained from the FTIR analysis.

Furthermore, the XRD patterns of PVDF/TPU/CB-PPy 38/62 vol% and 50/50 vol% compression molded composites are displayed in Figure 5. The results show that the addition of low amount of CB-PPy (i.e., 3% and 5%) slightly changes the diffraction patterns of the composites indicating a similar content of PVDF β phase in these materials. However, when higher amounts of CB-PPy (i.e., 6% and 10%) are added to the composites, more substantial changes are observed in the XRD patterns of the composites indicating that PVDF crystalline phases are modified. In fact, the peak at 17.7° corresponding the PVDF α phase disappears when 6% and 10% of CB-PPy are added in both composites, while the peak at 18.4°

TABLE 7 Summary of the piezoelectric coefficient (d_{33}) of PVDF/TPU/CB-PPy composites prepared by compression molding.

	d_{33} (pC/N)		
Sample	**1 N**	**2 N**	**4 N**
Neat PVDF	9.1 ± 6.9	4.4 ± 1.3	3.2 ± 1.1
Neat TPU	3.6 ± 1.4	3.6 ± 0.4	3.4 ± 0.2
PVDF/TPU 38/62 vol%			
% CB-PPy	1 N	2 N	4 N
0	2.8 ± 0.7	2.7 ± 0.6	2.8 ± 0.5
3	3.5 ± 0.3	3.2 ± 0.1	3.2 ± 0.1
5	4.9 ± 2.2	3.3 ± 1.3	3 ± 0.7
6	3.5 ± 1.7	3.5 ± 0.6	3.7 ± 0.2
7	7.6 ± 2.9	4.8 ± 1.5	3.7 ± 0.6
10	16.9 ± 7.6	7.5 ± 2.4	5.1 ± 1.1
15	20.2 ± 3.4	10.7 ± 2	6.4 ± 0.7
PVDF/TPU 50/50 vol%			
% CB-PPy	1 N	2 N	4 N
0	3 ± 0.8	3.1 ± 0.3	3.1 ± 0.1
1	5.3 ± 2.1	3.9 ± 0.9	3.3 ± 0.3
2	3.7 ± 0.6	3.2 ± 0.1	3.1 ± 0.1
3	3.4 ± 0.6	3.3 ± 0.3	3.2 ± 0.1
5	3 ± 1.1	3.7 ± 1.4	3.3 ± 0.3
6	6 ± 2.9	3.7 ± 1.2	3.5 ± 0.4
10	12.2 ± 4.3	7 ± 1.9	5.1 ± 1.2

Abbreviations: PVDF, poly(vinylidene fluoride); TPU, thermoplastic polyurethane.

significantly decreases in PVDF/TPU/CB-PPy 50/50 vol% composites. Moreover, the peak at 26.6° decreases when 6% of CB-PPy is added to PVDF/TPU/CB-PPy 38/62 vol% and practically disappear when 10% of CB-PPy is added to the composite. For PVDF/TPU/CB-PPy 50/50 vol% composites, this peak nearly disappear when 6% and 10% of CB-PPy are added. Those results are also in agreement to the FTIR spectra of the composites.

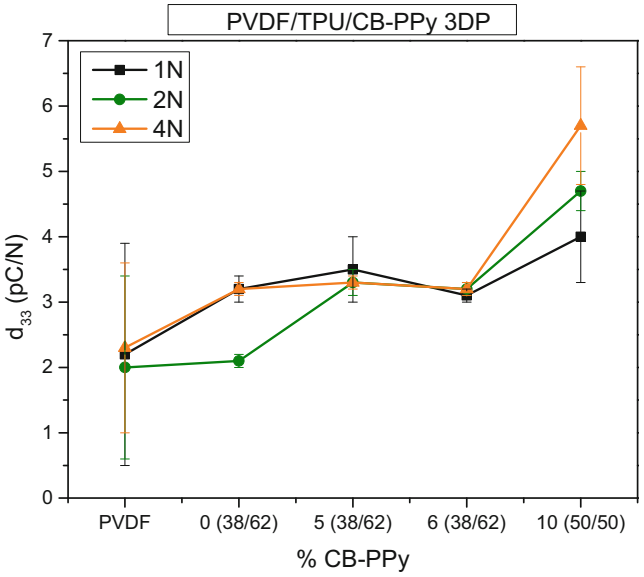

FIGURE 9 Piezoelectric coefficient (d_{33}) of PVDF/TPU/CB-PPy 3D printed composites. PVDF, poly(vinylidene fluoride); TPU, thermoplastic polyurethane

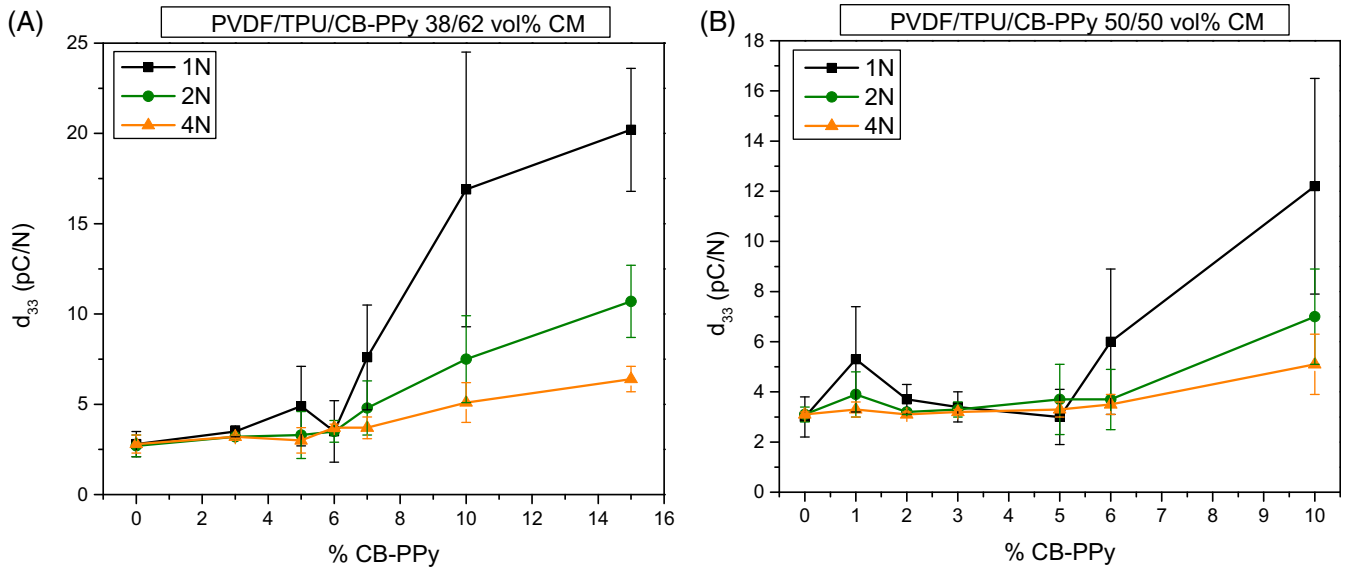

FIGURE 8 Piezoelectric coefficient (d_{33}) of (A) PVDF/TPU/CB-PPy 38/62 vol% and (B) PVDF/TPU/CB-PPy 50/50 vol% compression molded composites. PVDF, poly(vinylidene fluoride); TPU, thermoplastic polyurethane

The XRD patterns of the 3D printed composites were also evaluated and they are displayed in Figure 6. It is possible to observe some small changes when comparing the diffraction patterns of the 3D printed samples to the diffraction patterns of the same composites prepared by compression molding, thus indicating that the printing process may affect the crystalline phases of PVFD, as already discussed in the FTIR section.

3.4 | Piezoelectric d_{33} constant

The piezoelectric coefficient (d_{33}) was measured in order to investigate the relationship between the content of PVDF β phase in the composites and their piezoelectric responses. The d_{33} values for the neat polymers are displayed in Figure 7 and the d_{33} coefficients with the application of 1, 2, and 4 N of the static force for the neat polymers and the compression molded PVDF/TPU/CB-PPy composites are summarized in Table 7.

For the neat polymers, the results show that PVDF has better piezoelectric properties with respect to TPU, as expected. Regarding the PVDF/TPU/CB-PPy composites, Figure 8 and Table 7 show that although the piezoelectric responses is generally poor for the analyzed samples, when high quantities of the conductive filler are added to the composites a noticeable improvement in the piezoelectric coefficient can be detected. In fact, the piezoelectric responses significantly increase when the CB-PPy concentration overpasses the piezoelectric threshold value of 6% for PVDF/TPU/CB-PPy 38/62 vol% and 7% for PVDF/TPU/CB-PPy 50/50 vol%. The highest values of d_{33} are achieved with the addition of 15% of CB-PPy in PVDF/TPU/CB-PPy 38/62 vol% composites and 10% of CB-Py in PVDF/TPU/CB-PPy 50/50 vol% composites.

Moreover, it can be observed that the error bars are considerably large when static clamping force is 1 N. It may be related to non-homogeneity of samples or to non-optimal clamping, which can induce to imprecisions during the measurements. On the other hand, when the clamping force is increased to 2 N and 4 N, the error bars substantially decrease. However, a flattening can be observed in the d_{33} curves when the static force is raised to 4 N because the clamping force is probably too high for soft polymers and thin samples causing high sample deformation.[39–41]

Furthermore, the d_{33} constant was also measured for the specimens prepared by FFF. Figure 9 presents the d_{33} values of 3D printed samples showing that very low piezoelectric response was found for the 3D printed composites. Moreover, the concentration of CB-PPy in the 3D

TABLE 8 $F(\beta)$% and piezoelectric coefficient (d_{33}) of compression molded for PVDF/TPU/CB-PPy composites applying 1 N of static force.

PVDF/TPU/CB-PPy 38/62 vol%		
CB-PPy (%)	**$F(\beta)$ (%)**	**d_{33} (pC/N)**
0	41	2.8
3	41	3.5
6	50	3.5
10	61	16.9
PVDF/TPU/CB-PPy 50/50 vol%		
CB-PPy (%)	**$F(\beta)$ (%)**	**d_{33} (pC/N)**
0	33	3
3	32	3.4
6	52	6
10	57	12.2

Abbreviations: PVDF, poly(vinylidene fluoride); TPU, thermoplastic polyurethane.

	CM		**3D**	
Sample	**$F(\beta)$ (%)**	**d_{33} (pC/N)**	**$F(\beta)$ (%)**	**d_{33} (pC/N)**
PVDF	31	9.1 ± 6.9	32	2.2 ± 1.7
PVDF/TPU 38/62 vol%				
CB-PPy (%)	$F(\beta)$ (%)	d_{33} (pC/N)	$F(\beta)$ (%)	d_{33} (pC/N)
0	41	2.8 ± 0.7	37	3.2 ± 0.2
5	45	4.9 ± 2.2	43	3.5 ± 0.5
6	50	3.5 ± 1.7	43	3.1 ± 0.1
PVDF/TPU 50/50 vol%				
CB-PPy (%)	$F(\beta)$ (%)	d_{33} (pC/N)	$F(\beta)$ (%)	d_{33} (pC/N)
10	57	12.2 ± 4.3	49	4 ± 0.7

Abbreviations: PVDF, poly(vinylidene fluoride); TPU, thermoplastic polyurethane.

TABLE 9 Comparison of $F(\beta)$% and the piezoelectric coefficient (d_{33}) between compression molded (CM) and 3D printed (3D) specimens applying 1 N of static force.

printed composites does not significantly affect the piezoelectric response of the materials. In fact, even samples with high amount of CB-PPy (i.e., 6% and 10%) have not exhibited a substantial improvement in the piezoelectric coefficient values.

Additionally, in order to evaluate the relationship between the content of PVDF β phase in the composites and their piezoelectricity, Table 8 presents the values of $F(\beta)$ and d_{33} for compression molded PVDF/TPU/CB-PPy composites. Generally, the piezoelectric constant increased with the percentage of β phase for 38/62 vol% and 50/50 vol% composites. In addition, samples with more than 6% of CB-PPy have shown higher β phase content, thus higher values of d_{33}, endorsing the claim that the addition of high amount of CB-PPy was capable of assist the PVDF phase transformation.

Moreover, Table 9 presents a comparison of the $F(\beta)$ and d_{33} values between compression molded and 3D printed specimens. As discussed before, the FFF process leads to a decrease in the content of β phase and in the piezoelectric responses of the composites when compared to compression molded samples with same composition.

Overall, the results confirm that the piezoelectric properties of PVDF are associated to its β phase and that the compression molded composites have shown higher β phase content, thus better piezoelectric responses, confirming that the 3D printing process affect directly phase transformation of PVDF.

4 | CONCLUSIONS

In this study, the development of PVDF/TPU composites filled with CB doped with polypyrrole to increase the content of PVDF β phase and to enhance the piezoelectric properties of the composites was proposed. The piezoelectric responses, crystallinity and phase transformation of PVDF in compression molded and 3D printed PVDF/TPU/CB-PPy composites were investigated.

According to the results, the addition of TPU to PVDF can assist the crystallization of PVDF chains increasing degree of crystallinity and content of β phase in PVDF. Furthermore, the results show that although the addition of CB-PPy in the composites reduces the degree of crystallinity of PDVF, the percentage of PVDF β phase in the final materials is increased, however, it is more evident in samples with filler concentration higher than 6%. The addition of CB-PPy higher than 6%–7% seems to have a significant effect also on the piezoelectric coefficient (d_{33}) of compression molded samples. In addition, specimens prepared via FFF displayed lower content β phase in PVDF when compared to compression molded samples with same composition. As expected, 3D printed samples also presented lower piezoelectric responses when compared to compression molded composites with composition.

Overall, the piezoelectric responses of all composites increased with the percentage of PVDF β phase and the 3D printing process affected directly the phase transformation of PVDF and the piezoelectric response of the materials.

ACKNOWLEDGMENTS

This research has been funded by the Italian Ministry for University and Research (MUR) through the "Departments of Excellence" 2018-2022 program and Mayara Cristina Bertolini is supported by the "Departments of Excellence" grant L.232/2016. This work was also supported by the "Conselho Nacional de Desenvolvimento Científico e Tecnológico (CNPq)," Brazil.

DATA AVAILABILITY STATEMENT

The data that support the findings of this study are available from the corresponding author upon reasonable request.

ORCID

Mayara C. Bertolini https://orcid.org/0000-0003-2852-5450

Nico Zamperlin https://orcid.org/0000-0003-1736-9843

REFERENCES

1. Shoorangiz M, Sherafat Z, Bagherzadeh E. CNT loaded PVDF-KNN nanocomposite films with enhanced piezoelectric properties. *Ceram Int*. 2022;48(11):15180-15188.
2. Wan Y, Wang Y, Guo CF. Recent progresses on flexible tactile sensors. *Mater Today Phys*. 2017;1:61-73.
3. Chang Y, Zuo J, Zhang H, Duan X. State-of-the-art and recent developments in micro/nanoscale pressure sensors for smart wearable devices and health monitoring systems. *Nanotechnol Precis Eng*. 2020;3(1):43-52.
4. Gao Y, Yu L, Yeo JC, Lim CT. Flexible hybrid sensors for health monitoring: materials and mechanisms to render wearability. *Adv Mater*. 2020;32(15):e1902133.
5. Al-Saygh A, Ponnamma D, AlMaadeed MA, Vijayan P, Karim A, Hassan MK. Flexible pressure sensor based on PVDF nanocomposites containing reduced graphene oxide-titania hybrid nanolayers. *Polymers (Basel)*. 2017;9(2).
6. Elnabawy E, Hassanain AH, Shehata N, et al. Piezoelastic PVDF/TPU Nanofibrous composite membrane: fabrication and characterization. *Polymers (Basel)*. 2019;11(10).
7. Tarbuttona J, Leb T, Helfrichb G, Kirkpatrickb M. Phase transformation and shock sensor response of additively manufactured piezoelectric PVDF. *Proc Manuf*. 2017;10:982-989.
8. Kirkpatrick MB, Tarbutton JA, Le T, Lee C. Characterization of 3D printed piezoelectric sensors: Determiniation of d_{33} in piezoelectric coefficient for 3D printed polyvinylidene fluoride sensors. *IEEE Sensors*. 2016;1-3.

9. Yuan X, Yan A, Lai Z, et al. A poling-free PVDF nanocomposite via mechanically directional stress field for self-powered pressure sensor application. *Nano Energy*. 2022;98:107340.
10. Yan J, Liu M, Jeong YG, et al. Performance enhancements in poly(vinylidene fluoride)-based piezoelectric nanogenerators for efficient energy harvesting. *Nano Energy*. 2019;56:662-692.
11. Kim H, Johnson J, Chavez LA, Garcia Rosales CA, Tseng TLB, Lin Y. Enhanced dielectric properties of three phase dielectric MWCNTs/BaTiO3/PVDF nanocomposites for energy storage using fused deposition modeling 3D printing. *Ceram Int*. 2018;44(8):9037-9044.
12. Fakhri P, Mahmood H, Jaleh B, Pegoretti A. Improved electroactive phase content and dielectric properties of flexible PVDF nanocomposite films filled with Au- and Cu-doped graphene oxide hybrid nanofiller. *Synth Met*. 2016;220:653-660.
13. Behera M. Study of optical, thermal, mechanical and microstructural properties of fullerene/poly (vinylidene fluoride) polymer nanocomposites. *Biointerface Res Appl Chem*. 2022;13(2):121.
14. Seena M, Jan H, Prasad V. Dielectric properties of hot-pressed poly(vinylidene fluoride)/functionalized carbon nanotube composites. *Mater Chem Phys*. 2022;285:126134.
15. Wu CM, Chou MH. Acoustic–electric conversion and piezoelectric properties of electrospun polyvinylidene fluoride/silver nanofibrous membranes. *Express Polym Lett*. 2020;14(2):103-114.
16. Chen C, Cai F, Zhu Y, et al. 3D printing of electroactive PVDF thin films with high β-phase content. *Smart Mater Struct*. 2019;28(6):065017.
17. Kim H, Torres F, Villagran D, Stewart C, Lin Y, Tseng TLB. 3D printing of $BaTiO_3$/PVDF composites with electric in situ poling for pressure sensor applications. *Macromol Mater Eng*. 2017;302(11):1700229.
18. Kim H, Fernando T, Li M, Lin Y, Tseng TLB. Fabrication and characterization of 3D printed $BaTiO_3$/PVDF nanocomposites. *J Compos Mater*. 2017;52(2):197-206.
19. You M-H, Wang XX, Yan X, et al. A self-powered flexible hybrid piezoelectric–pyroelectric nanogenerator based on non-woven nanofiber membranes. *J Mater Chem A*. 2018;6(8):3500-3509.
20. Wu L, Yuan W, Hu N, et al. Improved piezoelectricity of PVDF-HFP/carbon black composite films. *J Phys D Appl Phys*. 2014;47(13):135302.
21. Dhatarwal P, Sengwa RJ. Tunable β-phase crystals, degree of crystallinity, and dielectric properties of three-phase PVDF/PEO/SiO_2 hybrid polymer nanocomposites. *Mater Res Bull*. 2020;129:110901.
22. Lederle F, Härter C, Beuermann S. Inducing β phase crystallinity of PVDF homopolymer, blends and block copolymers by anti-solvent crystallization. *J Fluor Chem*. 2020;234:109522.
23. Hari MA, Karumuthil SC, Varghese S, Rajan L. Performance enhancement of flexible and self-powered PVDF-ZnO based tactile sensors. *IEEE Sensors J*. 2022;22(10):9336-9343.
24. Dios JR, Garcia-Astrain C, Gonçalves S, Costa P, Lanceros-Méndez S. Piezoresistive performance of polymer-based materials as a function of the matrix and nanofiller content to walking detection application. *Compos Sci Technol*. 2019;181:107678.
25. Bencomo JA, Iacono ST, McCollum J. 3D printing multifunctional fluorinated nanocomposites: tuning electroactivity, rheology and chemical reactivity. *J Mater Chem A*. 2018;6(26):12308-12315.
26. Momenzadeh N, Stewart CM, Berfield T. Conference Proceedings of the Society for Experimental Mechanics Series. In: Kramer S et al., eds. *Mechanical and thermal characterization of fused filament fabrication polyvinylidene fluoride (PVDF) printed composites, in mechanics of additive and advanced manufacturing*. Springer; 2019:59-65.
27. Chatham CA, Zawaski CE, Bobbitt DC, Moore RB, Long TE, Williams CB. Semi-crystalline polymer blends for material extrusion additive manufacturing printability: a case study with poly(ethylene terephthalate) and polypropylene. *Macromol Mater Eng*. 2019;304(5):1800764.
28. Bera M, Saha U, Bhardwaj A, Maji PK. Reduced graphene oxide (RGO)-induced compatibilization and reinforcement of poly(vinylidene fluoride) (PVDF)—thermoplastic polyurethane (TPU) binary polymer blend. *Appl Polym*. 2019;136(5):47010.
29. Ma H, Xiong Z, Lv F, Li C, Yang Y. Rheological behavior and morphologies of reactively compatibilized PVDF/TPU blends. *Macromol Chem Phys*. 2011;212(3):252-258.
30. Bertolini MC, Dul S, Barra GMO, Pegoretti A. Poly(vinylidene fluoride)/thermoplastic polyurethane flexible and 3D printable conductive composites. *J Appl Polym Sci*. 2020;138(17):50305.
31. Bertolini MC, Dul S, Lopes Pereira EC, Soares BG, Barra GMO, Pegoretti A. Fabrication and characterization of piezoresistive flexible pressure sensors based on poly(vinylidene fluoride)/thermoplastic polyurethane filled with carbon black-polypyrrole. *Polym Compos*. 2021;42:6621-6634.
32. Wu L, Jing M, Liu Y, et al. Power generation by PVDF-TrFE/graphene nanocomposite films. *Compos Part B Eng*. 2019;164:703-709.
33. Georgousis G, Pandis C, Kalamiotis A, et al. Strain sensing in polymer/carbon nanotube composites by electrical resistance measurement. *Compos Part B Eng*. 2015;68:162-169.
34. Atanassov A, Kostov G, Kiryakova D, Borisova-Koleva L. Properties of clay nanocomposites based on poly(vinylidene fluoride-co-hexafluoropropylene). *J Thermoplast Compos Mater*. 2012;27(1):126-141.
35. Merlini C, Barra GMO, Medeiros Araujo T, Pegoretti A. Electrically pressure sensitive poly(vinylidene fluoride)/polypyrrole electrospun mats. *RSC Adv*. 2014;4(30):15749-15758.
36. Ramoa SDAS, Barra GMO, Merlini C, Livi S, Soares BG, Pegoretti A. Novel electrically conductive polyurethane/montmorillonite-polypyrrole nanocomposites. *Express Polym Lett*. 2015;9(10):945-958.
37. Gregorio R Jr, Nociti NCPS. Effect of PMMA addition on the solution cristalizattion of alpha and beta phase of PVDF. *J Phys D Appl Phys*. 1995;28:432-436.
38. Kennedy ZC, Christ JF, Evans KA, et al. 3D-printed poly(vinylidene fluoride)/carbon nanotube composites as a tunable, low-cost chemical vapour sensing platform. *Nanoscale*. 2017;9(17):5458-5466.

39. Almusallam A, Yang K, Zhu D, et al. Clamping effect on the piezoelectric responses of screen-printed low temperature PZT/polymer films on flexible substrates. *Smart Mater Struct*. 2015;24(11):115030.
40. Al Ahmad M, Coccetti F, Plana R. The Effect of Substrate Clamping on Piezoelectric Thin-Film Parameters in Proceedings of Asia-Pacific Microwave Conference. 2007.
41. Torah RN, Beeby SP, White NM. Experimental investigation into the effect of substrate clamping on the piezoelectric behaviour of thick-film PZT elements. *J Phys D Appl Phys*. 2004;37(7):1074-1078.

How to cite this article: Bertolini MC, Zamperlin N, Barra GMO, Pegoretti A. Development of poly(vinylidene fluoride)/thermoplastic polyurethane/carbon black-polypyrrole composites with enhanced piezoelectric properties. *SPE Polym*. 2023;4(4):143-155. doi:10.1002/pls2.10097